

# Quantum Monte Carlo Study of the Rabi-Hubbard Model

T. Flottat<sup>1</sup>, F. Hébert<sup>1</sup>, V.G. Rousseau<sup>2</sup>, and G.G. Batrouni<sup>1,3,4,5</sup>

<sup>1</sup>*UCA, CNRS, INLN; 1361 route des Lucioles, 06560 Valbonne, France*

<sup>2</sup>*Physics Department, Loyola University New Orleans, 6363 Saint Charles Ave., LA 70118, USA*

<sup>3</sup>*Institut Universitaire de France, 103 bd Saint-Michel, 75005 Paris, France,*

<sup>4</sup>*MajuLab, CNRS-UNS-NUS-NTU International Joint Research Unit UMI 3654, Singapore and*

<sup>5</sup>*Centre for Quantum Technologies, National University of Singapore; 2 Science Drive 3 Singapore 117542*

We study, using quantum Monte Carlo (QMC) simulations, the ground state properties of a one dimensional Rabi-Hubbard model. The model consists of a lattice of Rabi systems coupled by a photon hopping term between near neighbor sites. For large enough coupling between photons and atoms, the phase diagram generally consists of only two phases: a coherent phase and a compressible incoherent one separated by a quantum phase transition (QPT). We show that, as one goes deeper in the coherent phase, the system becomes unstable exhibiting a divergence of the number of photons. The Mott phases which are present in the Jaynes-Cummings-Hubbard model are not observed in these cases due to the presence of non-negligible counter-rotating terms. We show that these two models become equivalent only when the detuning is negative and large enough, or if the counter-rotating terms are small enough.

PACS numbers: 05.30.Jp, 05.30.Rt, 42.50.Pq

## I. INTRODUCTION

In recent years, the possibility to build [1, 2] elementary cavity quantum electrodynamics systems, whether formed by an atom in a cavity [3] or by a Josephson junction coupled to microwave photons on a chip [4], opened the perspective to construct new many body systems from such elementary building blocks.

The Jaynes-Cummings-Hubbard (JCH) model [5] is the simplest model describing such an array of coupled cavities. Each cavity consists of a two-level system (describing the atom or the junction) coupled to a unique mode of the cavity. The cavities are then coupled by tunneling of photons from one cavity to the next. In this many-cavity system, it was predicted that a phenomenon similar to a photon blockade [6] would take place, leading to a phase transition between a coherent state, where all the cavities are in phase, and an incoherent state where the number of excitations per cavity is quantized, reminiscent of the Mott-superfluid transition observed in the bosonic Hubbard model [7–13]. Non equilibrium properties of such systems have also been extensively discussed [14, 15].

In the JCH model description of such a system, the total number of excitons,  $N$ , the sum of the number of photons  $N_l$  and of excited atoms (also referred to as spins)  $N_s$ , is a conserved quantity. However, a complete description of the interaction between the two-level system and the photon field should include, as described by the Rabi Hamiltonian [16], so-called counter-rotating (CR) terms that do not conserve the number of excitations. Neglecting these terms, which is generally called the rotating wave approximation (RWA), is generally valid due to the very small values of the coupling  $g$  between the field and the material device. Compared to the energy of a photon  $\omega_l$ ,  $g$  generally ranges from  $g/\omega_l \simeq 10^{-7}$  in cavity quantum electrodynamics (QED) experiments up

to  $g/\omega_l \simeq 10^{-3}$  in circuit QED [2].

However, it was recently remarked that, for larger values of  $g$ , these CR terms may modify deeply the physics of these systems [17–19]. In [18], Schiro *et al.* introduced the Rabi-Hubbard (RH) model, which is equivalent to the JCH model with the addition of counter-rotating terms, both in the interaction and the hopping terms. This model has different symmetry properties from the JCH model and consequently different transitions. The studies performed in [17–20] show that the RH model does not exhibit Mott insulating behavior, but rather an incoherent/coherent transition which resembles the superadiant transition of the Dicke model [21, 22]. The out of equilibrium behavior of the RH model has been recently studied in Ref.[23]. The related Dicke model and the nature of its transition are also the subject of intense research [22, 24–26]. Recent experiments show the breakdown of the RWA approximation by reaching an ultra strong coupling regime in circuit QED [27, 28] where  $g/\omega_l \simeq 10^{-1}$ .

In order to study the differences between the RH and JCH descriptions of these systems, we will use exact quantum Monte Carlo (QMC) simulations. Whereas the JCH model has been studied with DMRG [9] and QMC [13] the RH model has mostly been studied with mean-field approximations [17–19]. Kumar *et al.* [20] mapped the RH model onto the quantum Ising model in the strong coupling limit ( $g/\omega_l > 1$ ) and compared their results with DMRG simulations. They found that the QPT of the RH model is well described by the dynamics of the quantum Ising model. However, their calculation was done with the number of photons per cavity restricted to be at most equal to 3. As we will see below, the number of photons per cavity can far exceed this value in the coherent phase. In addition, the DMRG calculation of Ref. [20] was done without the CR terms in the hopping. Below, we will study the effect of these terms.

The JCH and RH models we will study in this paper are but two of a very wide variety of related models describing a large spectrum of interesting physical situations of current interest. For example, Ref. [29] introduces a model of spins coupled to photons which are exchanged at all distances and where the photon band is *flat*, which is a key difference with the model we address here. Another interesting class of models is that where the band is not flat and where, in addition, spin-photon coupling is mode dependent and chosen to lead to an Ohmic spectral density at low enough frequencies [30]. These models can also be studied with the QMC algorithm we use in this paper.

In Section II, we review the model, the technique used to simulate it and the physical quantities of interest for this study. In Section III, we present the phase diagram of the model and compare it with previously known results, focusing on the case where the detuning is zero. In Section IV, we discuss in more detail the importance of the counter-rotating terms and their effects.

## II. MODELS AND TECHNIQUES

We study the Rabi-Hubbard model on a one-dimensional periodic chain with  $L$  sites. Each site of the chain, labelled with index  $i$ , represents a cavity (Fig. 1). In each cavity there is a two-level atom represented as a spin-1/2 and we consider only one photon mode per cavity. The atom is coupled to the mode with the Rabi-Hamiltonian [16]. The sites are coupled to each other by a photon hopping term connecting near neighbor cavities via the tunnel effect. The Rabi-Hubbard (RH) Hamiltonian governing this system is [18]

$$\begin{aligned}
 H = & -J \sum_i (a_i + a_i^\dagger)(a_{i+1} + a_{i+1}^\dagger) \\
 & + \sum_i (\omega_s \sigma_i^+ \sigma_i^- + \omega_l a_i^\dagger a_i) \\
 & + g \sum_i (\sigma_i^- + \sigma_i^+)(a_i + a_i^\dagger)
 \end{aligned} \quad (1)$$

The  $a_i(a_i^\dagger)$  describes the destruction (creation) of photons in the  $i$ -th cavity. The  $\sigma_i$  operators describe the two-level atoms. The first term in Eq.(1) describes the hopping of photons between cavities; the second term, which is diagonal, describes the energies of the photons and the excited atomic states. The third term describes the exchange between the atom and the photons field. We will call  $\delta = \omega_a - \omega_l$  the detuning between the atomic and light frequencies

Written in this form, the Hamiltonian includes counter-rotating terms (CR): terms which create two photons ( $a_i^\dagger a_{i+1}^\dagger$ ) in the first line of Eq.(1) or which simultaneously excite a spin and create a photon ( $\sigma_i^+ a_i^\dagger$ ) in the third, and their Hermitian conjugates. This last term is often neglected in the treatment of the Rabi model as it

couple states with different diagonal energies. The non-rotating terms in the hopping part of the Hamiltonian are probably not physical but were studied in [18] and allow us to study the effects of two different non rotating terms. Ignoring these terms in Eq.(1), what is generally called the rotating wave approximation (RWA), transforms the model into the Jaynes-Cummings-Hubbard (JCH) Hamiltonian [5]. There is an important qualitative difference between these models. The JCH model conserves the number of excitations  $N = N_s + N_l$  and has U(1) symmetry whereas the RH model does not have such a conservation law and has a simpler  $Z_2$  symmetry.

To study the differences between the JCH and RH models, we perform exact numerical simulations using the Stochastic Green Function (SGF) quantum Monte Carlo algorithm [31, 32]. This numerical technique is able to tackle the non-conservation of the number of excitations and the large number of photons present in the RH model. This allowed us the study its phase diagram and simulate sizes up to  $L = 30$  sites and inverse temperatures  $\beta\omega_l \simeq 20$ . We chose to study a one dimensional lattice where results can easily be compared with DMRG studies of the JCH [9] and RH [20] models and because of the limited number of sites we can study. To study in more details the effects of the CR terms, we generalize slightly the forms of the parameters  $g$  and  $J$ . The hopping term will then be replaced with

$$- \sum_i J_r (a_i a_{i+1}^\dagger + \text{h.c.}) + J_{cr} (a_i a_{i+1} + \text{h.c.}), \quad (2)$$

and the Rabi term with

$$\sum_i g_r (\sigma_i^+ a_i + \sigma_i^- a_i^\dagger) + g_{cr} (\sigma_i^+ a_i^\dagger + \sigma_i^- a_i), \quad (3)$$

where we introduce separate parameters for the rotating and counter-rotating terms ( $g_r, J_r$  and  $g_{cr}, J_{cr}$ , respectively).

We measure the number of photons  $N_l$  or the total number of excitations  $N$  and the corresponding densities  $n_l = N_l/L$  and  $n = N/L$ ; we also measure various Green functions

$$G_{\alpha\beta}(R) = \frac{1}{2L} \sum_i \langle \alpha_i \beta_{i+R} + \text{h.c.} \rangle \quad (4)$$

where  $\alpha$  and  $\beta$  are creation or destruction operators for the photons ( $a^\dagger$  or  $a$ ) or the spins ( $\sigma^+$  or  $\sigma^-$ ). This allows us to study the phase coherence of photons, spins and coherence between photons and spins. For example, we will measure the photon equal-time Green function

$$G_{a^\dagger a}(R) = \frac{1}{2L} \sum_i \langle a_i^\dagger a_{i+R} + a_{i+R}^\dagger a_i \rangle \quad (5)$$

This yields the photon condensate fraction,  $C_l$ , which is the order parameter for the phase coherence of photons:

$$C_l = \frac{\sum_R G_{a^\dagger a}(R)}{N_l}. \quad (6)$$

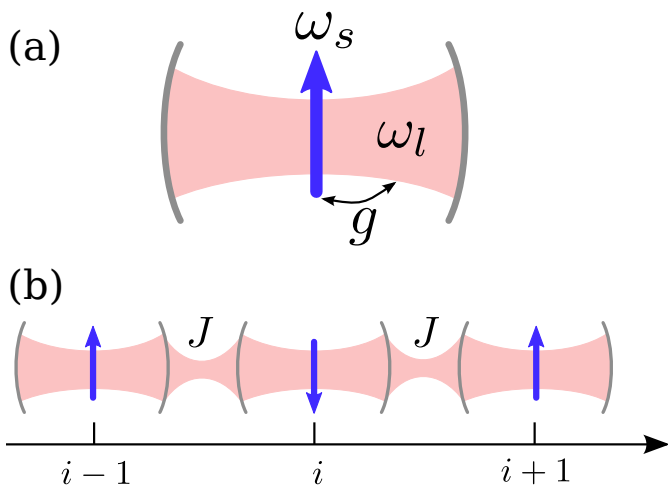


FIG. 1: (Color online) The Rabi model (a) describes the interaction of a two levels quantum system (here represented by a spin) with a mode of a photon field (here in pink). The Jaynes-Cummings or Rabi-Hubbard models describe the coupling of such Rabi cavities by tunnel effect of the photons between a cavity and the next.

Combining different spin-spin correlation functions such as

$$G_{\sigma^-\sigma^+}(R) = \frac{1}{2L} \sum_i \langle \sigma_i^- \sigma_{i+R}^+ + \sigma_{i+R}^- \sigma_i^+ \rangle, \quad (7)$$

we obtain the spin-spin correlation

$$C_s = \frac{1}{2L} \sum_i \langle \sigma_i^x \sigma_{i+L/2}^x \rangle \quad (8)$$

at the largest distance  $L/2$  in the system which exposes the coupling of the atoms via the photon field.

### III. PHASES AND PHASE DIAGRAM AT $\delta = 0$

We start with the Rabi-Hubbard model at  $\delta = 0$  and with:  $g_r = g_{cr} = g$  and  $J_r = J_{cr} = J$ . We take  $\omega_l = \omega_s = 1$  to fix the energy scale and we study the phase diagram as  $J/\omega_l$  is varied for a fixed value of  $g$ .

We observed, as predicted in [18], that the system undergoes an evolution from an incoherent phase, at low  $J$ , to a coherent one, at large  $J$ . The incoherent phase is characterized by exponential decay of all the Green functions with distance indicating the absence of long range and quasi-long range order in the system (Fig. 2, left). This means that the photons are not coherent at long distance and that the spins are also not ordered. The density of photons, equal to  $G_{a^\dagger a}(0)$ , is also small in this phase, of the order of  $3 \cdot 10^{-1}$  in the case presented here.

At large  $J$  we observe, on the contrary, a phase where all the Green functions remain non-zero at large distances (Fig. 2, right). The photons form a coherent field across the system and the spins adopt a ferromagnetic order

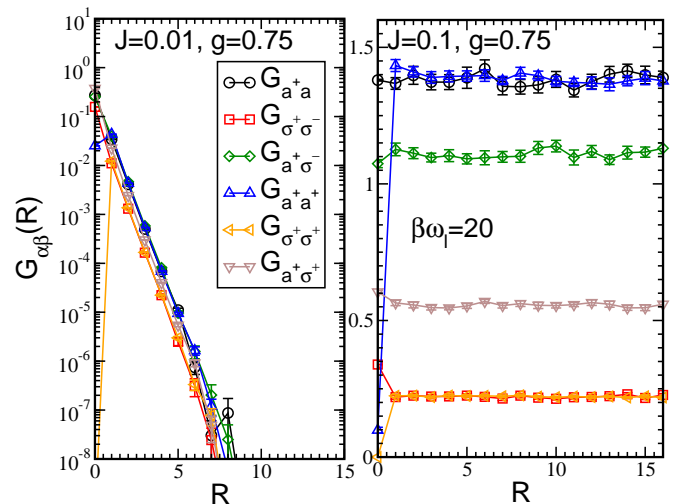


FIG. 2: (Color online) Green functions (Eq.(4)) as a function of distance in the incoherent (left) and coherent (right) phases. In the incoherent phase, all the Green functions decay exponentially. In the coherent phase, all the Green functions show a plateau behavior, reaching a constant value at long distance. This is due to the discrete symmetry of the Rabi-Hubbard model.

along the  $x$ -axis. The spins and photons are correlated with each other at long distances, as is shown by the behavior of mixed Green functions such as  $G_{a^\dagger \sigma^-}(R)$ . Finally, the density of photons becomes larger (around 1.4 in the present case) in this coherent phase.

To study the transition between the incoherent and coherent regimes for the photons, we will look at the evolution of the condensate fraction  $C_l$ . The value of  $C_l$  (Fig. 3) is not zero for small  $J$  while we observe that all the Green functions (see Fig. 2, left) decrease exponentially in this phase. We will show that this non-zero  $C_l$  is only a finite size effect.  $C_l$  increases as the system becomes coherent at larger  $J$ .

A striking feature is that  $C_l$  almost reaches its saturation value of unity for large  $J$  indicating that all the photons are condensed. This is atypical in one dimension, where one usually encounters quasi-condensation of the photons. In the present case, the condensation is due to the discrete  $Z_2$  symmetry of the RH model. This is also visible in the behavior of the Green functions in the coherent phase (Fig. 2, right) where all the Green functions reach plateaux with constant values at large distances, instead of the power law decay generally observed in one dimension. Another important feature is that we observe only the two phases, incoherent and coherent photon phases, with no sign of any Mott insulator where  $C_l$  would be zero for commensurate densities. This result confirms the mean field analysis of [18].

The spin-spin correlations  $C_s$  follow the behavior of the condensate fraction (Fig. 4): as the photons become coherent, the spins couple to the photon field and become ferromagnetic (or ferroelectric in terms of polarization of

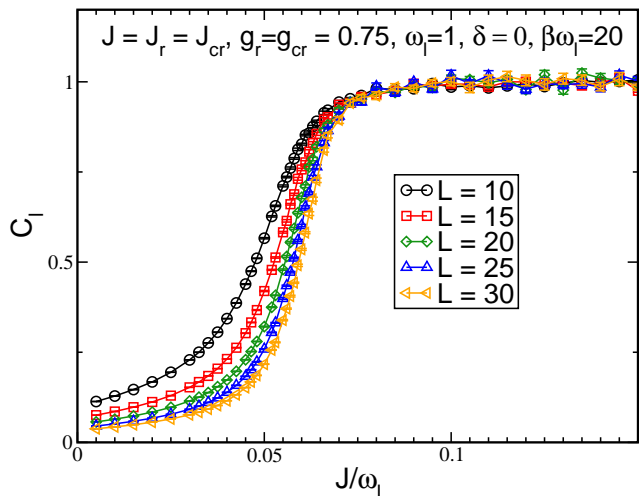


FIG. 3: (Color online) Condensate fraction  $C_l$  (Eq.(6)) of the photons as a function of  $J/\omega_l$  for detuning  $\delta = 0$ . The system undergoes a phase transition from an incoherent field to a coherent field as the coupling  $J$ .

the atoms). Once again, we find true long range order for the spin-spin correlations (Fig. 2) which tend to their saturated value of  $1/4$  when  $J/\omega_l$  becomes large. We observe that both  $C_l$  and  $C_s$  become large simultaneously, which suggests that there is no intermediate phase where one species is coherent while the other is not.

The transition is similar to the Dicke transition [22]. The main difference between the RH and Dicke models is that there are several in the former. However (Fig. 2, right)  $G_{a^\dagger a}(R)$  reaches a plateau at long distance. There is then a Bose condensation of the photons with a macroscopic occupation of the  $k = 0$  mode in Fourier space. Indeed, the number of photons  $N(k)$  occupying a Fourier mode of wave vector  $k$  is simply the Fourier transform of  $G_{a^\dagger a}(R)$ . Then, despite the fact that there are many photon modes, the system selects the lowest energy one when it becomes coherent and the resulting coherent phase is very similar to that in the Dicke system. Similarities between the JCH and Dicke model were discussed in [33].

To determine more precisely the transition point between the incoherent and coherent phases, we perform finite size scaling analysis [34]. This one-dimensional system has discrete  $Z_2$  symmetry and, consequently, its ground state quantum phase transitions belong to the classical two-dimensional Ising model universality class. The order parameter is  $\langle a \rangle = \sqrt{C_l}$  (or, equivalently, the magnetization of the spin along the  $x$ -axis). At the critical point, we expect the order parameter to scale like  $L^{-\beta_c/\nu_c}$  where  $\beta_c = 1/8$  and  $\nu_c = 1$  are the critical exponents. Hence,  $C_l L^{2\beta_c/\nu_c}$  is independent of  $L$  at the transition which allows us to determine the critical point  $J_c$  with good precision (Fig. 5). In addition, we confirmed (not shown here) the collapse of curves for different system sizes in the critical region by using the

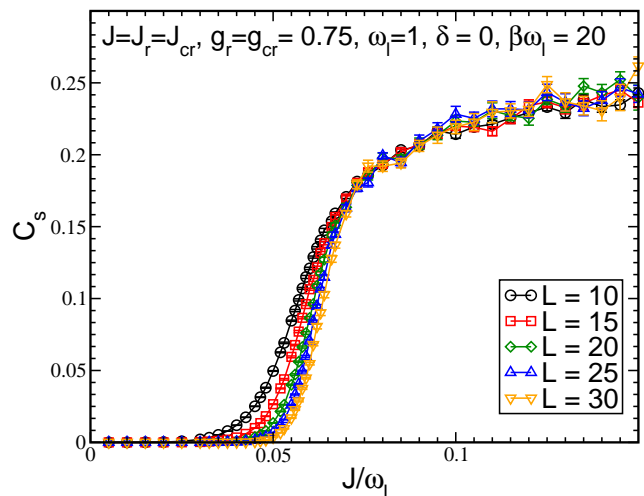


FIG. 4: (Color online) Spin-spin correlations  $C_s$  (Eq.(8)) at the maximum distance  $R = L/2$  as a function of  $J/\omega_l$  for detuning  $\delta = 0$  and for different sizes. As the photons become coherent (see Fig. 3), the system becomes “ferromagnetic”.

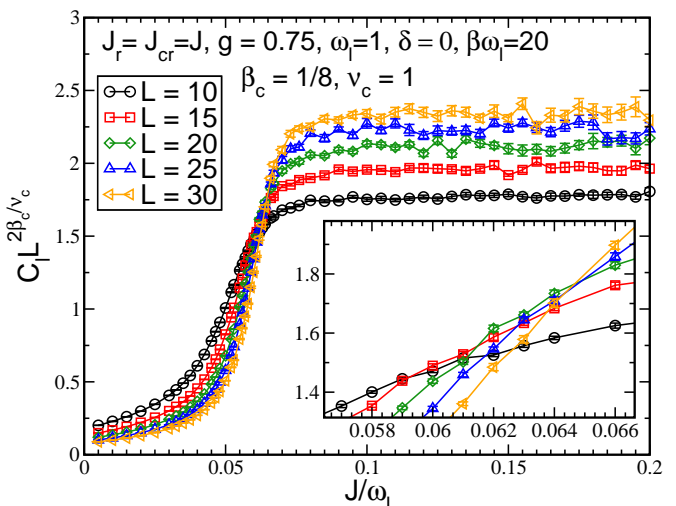


FIG. 5: (Color online) Finite size scaling analysis at the coherent/incoherent transition. We used the critical exponents of the 2D Ising universality class and observe, as expected, a universal crossing of the curves. Inset: Zoom on the transition region. For this value of  $g$ , the transition is located around  $J_c/\omega_l \simeq 0.062$ .

rescaled transition parameter  $(J - J_c)L^{1/\nu_c}$ . This confirms the two-dimensional Ising universality class of the transition. Performing such analysis for many different values of  $g$  allows us to determine the transition line between incoherent and coherent regions in the  $(J/\omega_l, g/\omega_l)$  plane.

We also analysed this transition by doing the mean-field (MF) analysis previously performed by Schiró *et al.* [19], which we briefly review here. As the kinetic terms are the only ones that couple sites, we can replace them,

for each site, with a coupling to an external homogeneous field  $\psi = \langle a_i \rangle$  for all  $i$ . We are then left with a collection of identical on-site MF Hamiltonians

$$H_i^{MF} = \omega_s \sigma_i^+ \sigma_i^- + \omega_l a_i^\dagger a_i + g (\sigma_i^+ + \sigma_i^-) (a_i + a_i^\dagger) - J_r (\psi^* a_i + \psi a_i^\dagger) - J_{cr} (\psi a_i + \psi^* a_i^\dagger). \quad (9)$$

These on-site Hamiltonians can be numerically diagonalized, in the standard way, by truncating a basis for a large enough number of photons and a self consistent solution is obtained when the mean value of  $a_i$  calculated in the ground state is equal to the field  $\psi$  inserted in the Hamiltonian. This also corresponds to a minimum value of the energy with respect to  $\psi$  as the method is variational.

To analyse the number of photons, we will now use an even simpler approximation, where we replace all photon operators  $a_i$  ( $a_i^\dagger$ ) by one c-number  $\psi$  ( $\psi^*$ ). This is a simple coherent state approach that should be valid in the coherent phase when the photon number is large enough to neglect fluctuations. Our problem is then reduced to simple MF Hamiltonians  $H_i^{SMF}$ , with only two states, describing independent spins coupled to the same perfectly coherent field,

$$H_i^{SMF} = \omega_s \sigma_i^+ \sigma_i^- + \omega_l |\psi|^2 + g (\sigma_i^+ + \sigma_i^-) (\psi + \psi^*) - 2J_r |\psi|^2 - J_{cr} (\psi^2 + (\psi^*)^2). \quad (10)$$

Due to the  $Z_2$  symmetry of the problem, the value of  $\psi$  that minimizes the energy can be chosen real and positive. Solving this two-state problem yields an expression for the transition line:

$$g = \frac{\sqrt{\omega_s(\omega_l - 2J_r - 2J_{cr})}}{2}, \quad (11)$$

and the density of photons in the coherent region,

$$n_l = |\psi|^2 = \frac{g^2}{(\omega_l - 2J_r - 2J_{cr})^2} - \frac{\omega_s^2}{16g^2}. \quad (12)$$

This reduces to  $n_l \simeq g^2/(\omega_l - 2J_r - 2J_{cr})^2$  for  $\psi \gg 1$  where the approximation should be valid. The number of photons will then diverge for  $\omega_l = 2(J_r + J_{cr})$  and the system becomes unstable for  $\omega_l$  smaller than this limit. Such instabilities are observed in photonic systems, for example in [10], when the chemical potential is large enough. Since  $\omega_l$  plays the role of a chemical potential in our system and as the number of excitations is not conserved, it is reasonable to find such a stability limit.

We used our QMC simulations to study the divergence of the number of photons as the instability point is approached, Fig. 6. We observe that  $n_l$  follows the simple MF result for the larger values of the photon density, which is expected since our approximation is not valid for small densities. It is very difficult numerically to get closer to the divergence point because the QMC becomes inefficient when there is a very large number of photons on a site (typically more than ten or twenty photons per

site). However, there is always a region where the MF behaviour is observed which confirms that the system is unstable below a given value of  $\omega_l$  ( $4J$  in the case of Fig. 6).

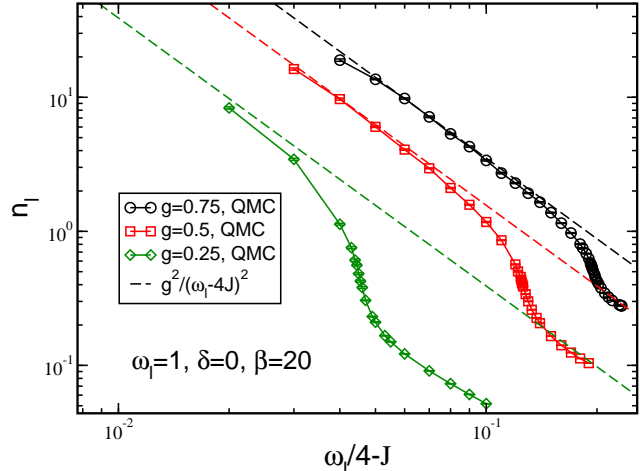


FIG. 6: (Color online) Comparison between the expected divergence of the density of photons,  $n_l$ , predicted with a simple mean field theory when  $J \rightarrow \omega_l/4$  and the QMC data. We find very good agreement for intermediate densities. At larger densities, the QMC becomes inefficient. Error bars are smaller than symbols.

As mentioned above, the finite size scaling analysis we performed for different values of  $g$ , allows us to determine the phase diagram in the  $(J/\omega_l, g/\omega_l)$  plane which we show in Fig. 7.

The MF results obtained in [18, 19] provide a qualitatively correct description of the transition line throughout the phase diagram. On the other hand, the simple ansatz Eq.(11) only works well for large  $J$ .

The absence of Mott insulating phases when the CR terms are taken into account, predicted in [19], is then also observed with our QMC simulations. However the model used so far [19] introduces unusual CR hopping, the  $J_{cr}$  term in Eq.(2). In order to investigate the effect of this term, we determined the phase diagram with  $(J_r \neq 0, J_{cr} = 0)$  while maintaining the CR term in the on-site exchange ( $g_r = g_{cr} = g$ ). We find a qualitatively similar phase diagram shown in Fig. 8. This demonstrates that, when the counter-rotating term is large enough, be it in the hopping or the exchange terms, the Mott insulating phases are suppressed. This can be understood by noting that the CR terms couple states with different numbers of excitations and, consequently, forbid the photon blockade [6] which is needed for the Mott phases to form [10].

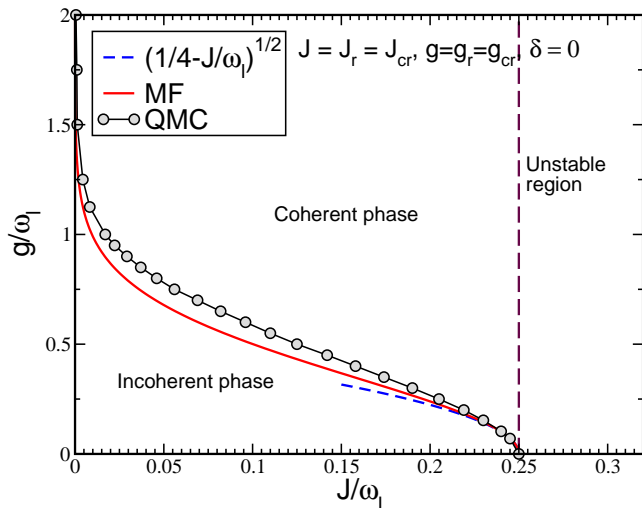


FIG. 7: (Color online) The phase diagram of the RH model at zero temperature with  $\delta = 0$  and  $J_r = J_{cr} = J$ . There is an unstable region for  $J/\omega_l > 1/4$ . The rest of the diagram is separated between a coherent (“superradiant”) region and incoherent (“insulating”) one. The continuous red line reproduces the limits found in the MF study of Schiro *et al.* [19] and the blue dashed line corresponds to the simple expression Eq.(11). Error bars are smaller than symbols.

#### IV. EFFECTS OF THE COUNTER-ROTATING TERMS

In the preceding section, we focused on the case with zero detuning, and found that the CR terms played a major role in the physics of our system and could not be neglected. This was expected as the values of  $g$  we used are large ( $g \simeq \omega_l$ ). We will now study cases where the detuning,  $\delta$ , is non zero or where  $g_{cr}$  is smaller than  $g_r$  to see if CR terms play an important part in these cases too. To simplify our study we will keep only the on-site CR term and set  $J_{cr} = 0$ . We will use the MF approximation that was used in [19], as it provides qualitatively correct results, as well as QMC.

We start by comparing the MF phase diagrams of the JCH and RH models at zero detuning, Fig. 9 (a), in the  $(J/g, (\mu - \omega_l)/g)$  plane, where  $\mu$  is the chemical potential. For the JCH model  $g_{cr} = 0$ ,  $g = g_r$  and we vary  $\mu - \omega_l$  which acts as the effective chemical potential for the photons in the grand canonical ensemble. For the RH model  $g_r = g_{cr} = g$  and we tune  $\omega_l$ , setting  $\mu = 0$ . The notion of canonical or grand canonical ensemble is not really pertinent for the RH model as the number of excitations is not a conserved quantity. As mentioned before, the models have very different phase diagrams. If we introduce positive detuning,  $\delta > 0$ , that is if  $\omega_s > \omega_l$ , we favor photon over spin excitations and this leads to similar differences between the two models as we encountered for  $\delta = 0$ .

However, if we introduce negative detuning  $\delta < 0$ , the physics of the two models becomes equivalent, as shown

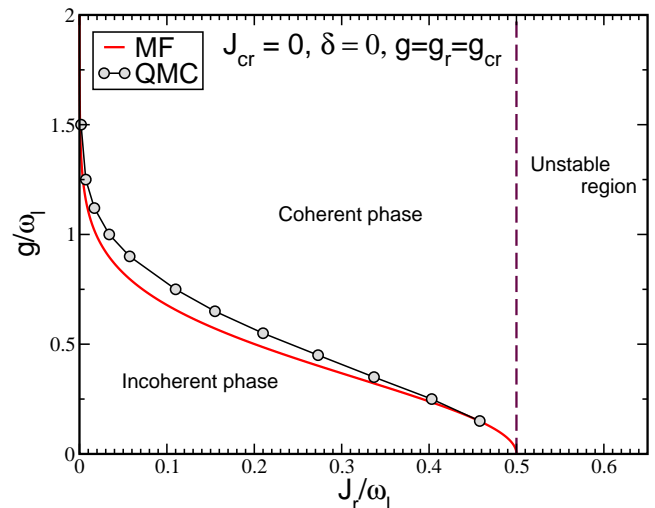


FIG. 8: (Color online) The phase diagram of the RH model with  $\delta = 0$ ,  $J_{cr} = 0$  and  $g = g_r = g_{cr}$  is very similar to Fig. 7. The continuous MF transition line was obtained with the same technique as in [19]. Whenever we have counter-rotating terms that are large enough, whether in the hopping term or in the exchange term between the spins and photons, we recover qualitatively the same diagram with only two phases (incoherent and coherent) and no Mott phases. Error bars are smaller than symbols.

in Fig. 9 (b) and (c). This is because  $\delta < 0$  favors atom excitations over photon creations and, then, reduces the possible fluctuations of the total number of excitations. In both models, we observe a region with no excitations, a Mott insulator phase for  $n = 1$ . However, we did not observe Mott phase at  $n = 2$  in the RH model. As  $|\delta|$  becomes larger (but always negative), the two phase diagrams become more similar as the MI phases with  $n > 1$  in the JCH model disappear and as the shape of the  $n = 1$  MI phase becomes more similar between the two models (Fig. 9 (c)).

To confirm this MF prediction, we show some QMC cuts in the phase diagram for negative detuning in Fig. 10. We observe the similarity of the behavior in this case with the  $n = 1$  Mott plateau visible in the JCH and the RH model, with similar width and the absence of a visible  $n = 2$  plateau. We then conclude that, for large values of  $g$ , the counter-rotating terms can be neglected only if there is a negative detuning that is large enough to overcome the coupling between states with different densities of excitations.

We now consider directly the effects of the counter-rotating term by tuning the value of  $g_{cr}$  keeping the other parameters fixed. We will use the zero detuned case (see Fig. 11). As expected, we find that for small values,  $g_{cr}/g_r = 0.01$ , the RH model gives results that are similar to the JCH model (treated in the canonical or grand canonical ensemble). However for  $g_{cr}/g_r = 0.1$ , the CR terms already have a strong effect and modify the physics by destroying the  $n = 1$  Mott phase. We see,

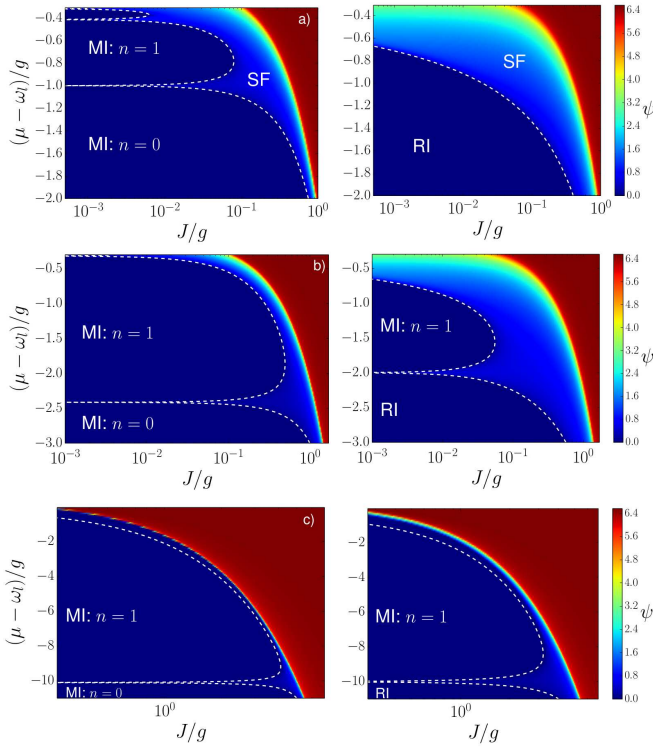


FIG. 9: (Color online) The MF phase diagrams of the JCH (left column) and RH (right column) models for different  $\delta$  at zero temperature. The color scale represents the real positive value of the MF order parameter  $\psi$ . (a) At  $\delta = 0$ , the phase diagrams are very different due to the degeneracy of the spin and photon energies. The JCH model shows several Mott insulator (MI) phases with different densities  $n$ , whereas the RH model only shows its incoherent/coherent transition. (b) As  $\delta/g = -2$  is decreased from zero, the MI phases with  $n > 1$  shrink in the JCH model whereas a small  $n = 1$  MI phase appear in the RH model. (c) At large  $\delta/g = -10$ , the two phase diagrams are almost equivalent with a single visible  $n = 1$  MI phase.

then, that the physics is very sensitive to the addition of small counter-rotating terms since, even with  $g_{cr}$  an order of magnitude smaller than  $g_r$ , we obtain a profound modification of the phase diagram.

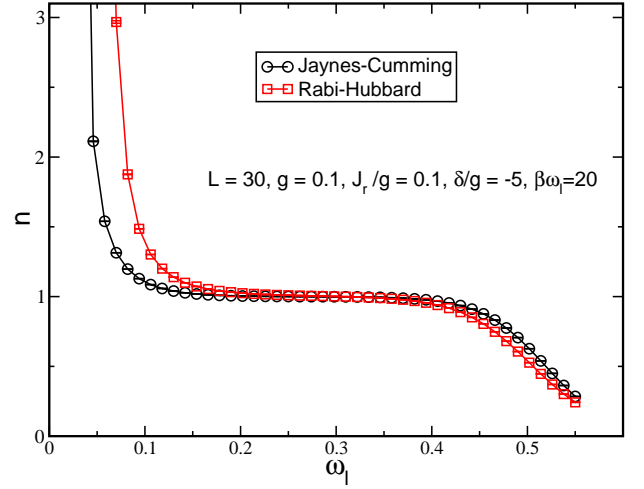


FIG. 10: (Color online) Density  $n$  of excitations versus  $\omega_l$  for a fixed  $g$  and  $J_r$  for the RH and JCH models using QMC. In both cases, we observe the Mott like plateau for a density  $n = n_s + n_l = 1$  of excitations with similar width. In both cases we do not observe the  $n = 2$  plateau. Error bars are smaller than symbols.

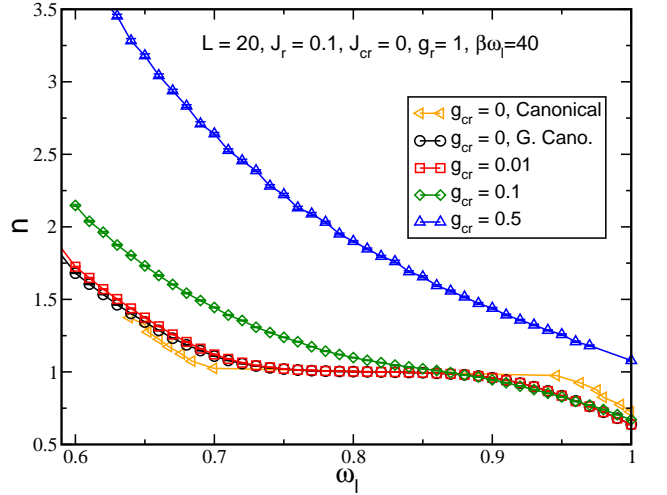


FIG. 11: (Color online) Number of excitations  $n$  as a function of  $\omega_l$  for different values of  $g_{cr}$  and fixed  $J_r$  and  $g_r$ , for the Jaynes-Cummings and Rabi-Hubbard models. We see that the two models give similar results for  $g_{cr}/g_r = 0.01$  but that the Mott plateau is destroyed even for  $g_{cr}/g_r = 0.1$ . Error bars are smaller than symbols.

## V. CONCLUSION

We studied the Rabi-Hubbard model and compared it with the Jaynes-Cummings model to see how the presence of counter-rotating terms, that involve fluctuations of the number of photons, changes the physics of said models.

For zero detuning, we observed that for large values

of the counter-rotating terms, be they in the hopping or on-site terms, the physics of the two models is completely different as the Mott phases present in the Jaynes-Cummings are destroyed in the RH model. We also observed that, due the discrete  $Z_2$  symmetry of the RH model, there is a transition between an incoherent phase and phase with true long range coherence similar to the Dicke transition, and we identified an unstable region in parameter space. These results are in good qualitative agreement with the MF results previously obtained by Schiro *et al.* [18, 19].

Exploring further, we identified two ways in which the effects of the counter-rotating terms can be reduced: by introducing a negative detuning or by directly making the counter-rotating parameter  $g_{cr}$  smaller. In both cases, the physics of the RH model approaches that of the JCH model.

By using arbitrarily large values of the counter-rotating terms, we depart from most experimental systems that have very small  $g$  parameters. Even with rather small values of  $g$ , the counter rotating terms can have a big impact on the phase diagrams, as is also observed in ultra strong coupling experiments [27, 28].

Another important effect in experiments is the presence of dissipative terms: losses from the cavity and

gains to compensate those. To obtain a strong coupling regime between the two-state system and the photons, these terms are generally small compared to  $g$ . However the system is driven out of equilibrium because of such effects.

Whereas we expect a Bose-Einstein condensation of photons at equilibrium, when the system is out of equilibrium, we expect phase coherence to appear through a lasing effect. The question of the difference between a laser and a Bose-Einstein condensate for photons is the subject of current debate [35], with the suggestion that there is a crossover between these two forms of coherent states. The QMC technique we use does not allow to study non Hermitian Hamiltonians but, including gain/loss terms that are Hermitian conjugates, we can address this question.

### Acknowledgments

The authors would like to thank B. Grémeaud and C. Miniatura for interesting discussions.

All the authors contributed equally to the paper.

- 
- [1] R.J. Schoelkopf and S.M. Girvin, *Nature* **451**, 664 (2008)
  - [2] A. Blais, R.-S. Huang, A. Wallraff, S. M. Girvin, and R. J. Schoelkopf, *Phys. Rev. A* **69**, 062320 (2004).
  - [3] S. Haroche and J.M. Raymond, *Exploring the Quantum : Atoms, Cavities and Photons*, Oxford Univ. Press (2006).
  - [4] A. Wallraff, D.I. Schuster, A. Blais, L. Frunzio, R.-S. Huang, J. Majer, S. Kumar, S.M. Girvin, and R.J. Schoelkopf, *Nature* **431**, 162 (2004).
  - [5] E.T. Jaynes and F.W. Cummings, *Proc. IEEE* **51**, 89109 (1963).
  - [6] K.M. Birnbaum, A. Boca, R. Miller, A.D. Boozer, T.E. Northup, and H.J. Kimble, *Nature* **436**, 87 (2005).
  - [7] A.D. Greentree, C. Tahan, J.H. Cole, and L.C.L. Hollenberg, *Nature Physics* **2**, 856 (2006).
  - [8] M. Hartmann, F. Brandao, and M.B. Plenio, *Nature Physics* **2**, 849 (2006).
  - [9] D. Rossini and R. Fazio, *Phys. Rev. Lett.* **99**, 186401 (2007).
  - [10] Jens Koch and Karyn Le Hur, *Phys. Rev. A* **80**, 023811 (2009).
  - [11] M.J. Hartmann, F.G.L.S Brandao, and M.B. Plenio, *Laser Photonics Rev.* **2**, 527 (2008).
  - [12] S. Schmidt and G. Blatter, *Phys. Rev. Lett.* **103**, 086403, (2009)
  - [13] J. Zhao, A.W. Sandvik, and K. Ueda, arXiv:0806.3603 [cond-mat.other] (2008).
  - [14] A. Tomadin, V. Giovannetti, R. Fazio, D. Gerace, I. Carusotto, H. E. Türeci, and A. Imamoglu, *Phys. Rev. A* **81**, 061801(R) (2010); *Phys. Rev. A* **82**, 019901 (2010).
  - [15] I. Carusotto and C. Ciuti, *Rev. Mod. Phys.* **85**, 299 (2013).
  - [16] I.I. Rabi, *Phys. Rev.* **49**, 324 (1936); **51**, 652 (1937).
  - [17] Hang Zheng and Yasutami Takada, *Phys. Rev. A* **84**, 043819 (2011).
  - [18] M. Schiró, M. Bordyuh, B. Öztop, and H.E. Türeci, *Phys. Rev. Lett.* **109**, 053601 (2012).
  - [19] M. Schiró, M. Bordyuh, B. Öztop and H.E. Türeci, *Journal of Physics B* **46**, 224021 (2013).
  - [20] B. Kumar and S. Jalal, *Phys. Rev. A* **88**, 011802(R) (2013).
  - [21] K. Hepp and E.H. Lieb, *Annals of Physics* **76**, 360 (1973).
  - [22] P. Rotondo, M. C. Lagomarsino, and G. Viola, *Phys. Rev. Lett.* **114**, 143601 (2015).
  - [23] M. Schiró, C. Joshi, M. Bordyuh, R. Fazio, J. Keeling, and H. E. Türeci, *Phys. Rev. Lett.* **116**, 143603 (2016).
  - [24] H. Zhu, G. Zhang, and H. Fan, *Scientific Reports* **6**, 19751 (2016).
  - [25] P. Nataf and C. Ciuti, *Nature Communications* **1**, 72 (2010).
  - [26] L.J. Zou, D. Marcos, S. Diehl, S. Putz, J. Schmiedmayer, J. Majer, and P. Rabl, *Phys. Rev. Lett.* **113**, 023603 (2014).
  - [27] T. Niemczyk, F. Deppe, H. Huebl, E.P. Menzel, F. Hocke, M.J. Schwarz, J.J. García-Ripoll, D. Zueco, T. Hümmer, E. Solano, A. Marx, and R. Gross, *Nature Physics* **6**, 772776 (2010).
  - [28] P. Forn-Díaz, J.J. García-Ripoll, B. Peropadre, M.A. Yurtalan, J.-L. Orgiazzi, R. Belyansky, C.M. Wilson, and A. Lupascu, prepublication arXiv:1602.00416 [quant-ph].
  - [29] A. Kurcz, A. Bermudez, and J.J. García-Ripoll, *Phys. Rev. Lett.* **112**, 180405 (2014).
  - [30] G. Díaz-Camacho, A. Bermudez, and J.J. García-Ripoll, *Phys. Rev. A* **93**, 043843 (2016).
  - [31] V. G. Rousseau, *Phys. Rev. E* **77**, 056705 (2008).



- [32] V. G. Rousseau, Phys. Rev. E **78**, 056707 (2008).
- [33] S. Schmidt, G. Blatter, and J. Keeling, J. Phys. B **46**, 224020 (2013).
- [34] H. Gould, J. Tobochnik, and W. Christian, *An Introduction to Computer Simulation Methods*, Addison-Wesley (2007).
- [35] J. Schmitt, T. Damm, D. Dung, F. Vewinger, J. Klaers, and M. Weitz, Phys. Rev. A **92**, 011602 (2015).